

CHEMISTRY

A European Journal

A Journal of



Accepted Article

Title: Robust Colloidal Nanoparticles of Pyrrolopyrrole Cyanines J-Aggregates with Bright Near Infrared Fluorescence in Aqueous Media: From Spectral Tailoring to Bioimaging Application

Authors: Cangjie Yang, Xiaochen Wang, Mingfeng Wang, Keming Xu, and Chenjie Xu

This manuscript has been accepted after peer review and appears as an Accepted Article online prior to editing, proofing, and formal publication of the final Version of Record (VoR). This work is currently citable by using the Digital Object Identifier (DOI) given below. The VoR will be published online in Early View as soon as possible and may be different to this Accepted Article as a result of editing. Readers should obtain the VoR from the journal website shown below when it is published to ensure accuracy of information. The authors are responsible for the content of this Accepted Article.

To be cited as: *Chem. Eur. J.* 10.1002/chem.201604741

Link to VoR: <http://dx.doi.org/10.1002/chem.201604741>

Supported by
ACES

WILEY-VCH

Robust Colloidal Nanoparticles of Pyrrolopyrrole Cyanines J-Aggregates with Bright Near Infrared Fluorescence in Aqueous Media: From Spectral Tailoring to Bioimaging Application

Cangjie Yang[†], Xiaochen Wang[†], Mingfeng Wang^{*}, Keming Xu, Chenjie Xu

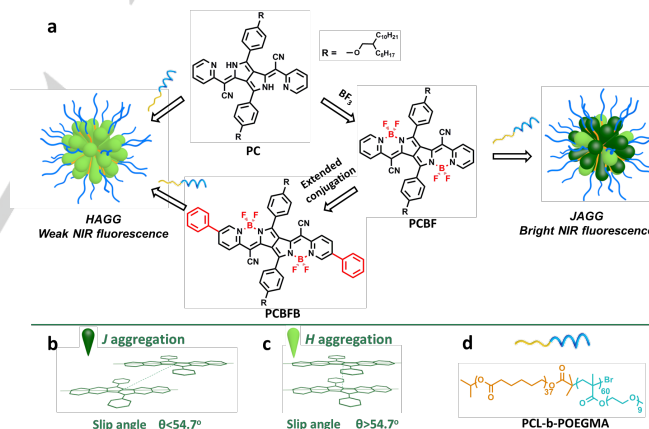
Abstract: We report a new class of colloidal nanoparticles called JAGG containing near-infrared fluorescent J-aggregates of pyrrolopyrrole cyanines (PPcys) stabilized by amphiphilic block copolymers in aqueous media. The formation of such JAGG can be tuned by the chemical structure of PPcys, the concentration of the chromophores inside the polymeric nanoparticles and ultrasonic treatment. These JAGG nanoparticles exhibit a narrow emission band at 773 nm, a fluorescence quantum yield comparable to that of indocyanine green, and significantly enhanced photostability that is ideal for long-term bioimaging.

Introduction

Fluorescence imaging *in vivo* in the near-infrared (NIR) window is important to enable deep tissue penetration with high optical contrast.^[1] To date there are only two clinically approved NIR fluorophores, indocyanine green (ICG) and methylene blue (MB), both of which are small molecules that can be rapidly excreted during circulation in physiological systems.^[2] In contrast to small molecular imaging probes, fluorescent nanoparticles (NPs) with sizes in the range of 10-100 nm usually show prolonged intracellular retention and enhanced permeation retention (EPR) effect,^[3] making them suitable for long term cell tracking^[4] and tumor targeting.^[5] One common strategy to prepare fluorescent colloidal NPs is to encapsulate the molecular fluorophores in a polymer matrix. However, the significant fluorescence (FL) quenching caused by the intermolecular aggregation of most organic fluorophores within NPs remains a challenge for bioimaging, with an exception of a group of special chromophores with strong emission in aggregated state^[6] and a series of fluorescent dyes covalently tethered with polymers.^[4b, 7]

Since the first discovery in 1936 by Jelley and Scheibe,^[8] J-aggregates (also called Scheibe aggregates), which exhibit strongly red-shifted light absorption and a nearly resonant

fluorescence, have attracted considerable attention for various applications.^[9] Such a resonant fluorescence band of J-aggregates with quite narrow bandwidth is highly desirable for simultaneous detection of multiple targets to minimize the spectral overlapping and interference. However, the bioimaging application of existing J-aggregates of dyes is limited by relatively low FL quantum yield, short emission wavelength and poor solubility in aqueous media. For instance, J-aggregates of ICG associated by van der Waals forces in water have been observed.^[9c, 10] But the colloidal stability of these aggregates without stabilization by surfactants was susceptible to changes of environmental factors such as concentration, ionic strength, and temperature. Recently, Zheng and coworkers^[11] reported that porphyrin J-aggregates formed in synthetic liposomes (also called porphysomes) showed dual photoacoustic and fluorescent properties for cancer imaging applications. Würthner and coworkers^[12] reported the J-type aggregation of H-bonding perylene bisimide derivatives with far-red fluorescence and high quantum yield, close to unity. But such self-assembly took place in nonpolar solvents which are not suitable for bioimaging.



Scheme 1 Schematic diagram of encapsulation of the PPcy derivatives into H-type and J-type aggregated nanoparticles (HAGG and JAGG): (a) molecular structures of PC, PCBF, PCBFB and the routes to formation of JAGG and HAGG nanoparticles; (b-c) schematic representation of J-aggregate (b) and H-aggregate (c); (d) chemical structure of the amphiphilic block copolymer PCL-b-POEGMA.

Herein, we present colloidal NPs of J-aggregates (denoted as JAGG) in water with bright NIR fluorescence and narrow bandwidth for bioimaging applications. The key component of the JAGG is a brightly fluorescent molecule, PCBF (as shown in Scheme 1), a pyrrolopyrrole cyanines (PPcy) derivative. PPcys containing a pyrrolopyrrole unit as the central element of a cyanine-type chromophore with emission in the NIR region up to 1000 nm and higher quantum yields than those of other organic NIR dyes were previously reported by Ficscher and coworkers.^[13]

[*] C. Yang,^[†] Dr. X. Wang,^[†] Prof. Dr. M. Wang, Dr. K. Xu, Prof. Dr. C. Xu
School of Chemical and Biomedical Engineering
Nanyang Technological University
62 Nanyang Drive, Singapore 637459, Singapore
E-mail: mfwang@ntu.edu.sg (MW)

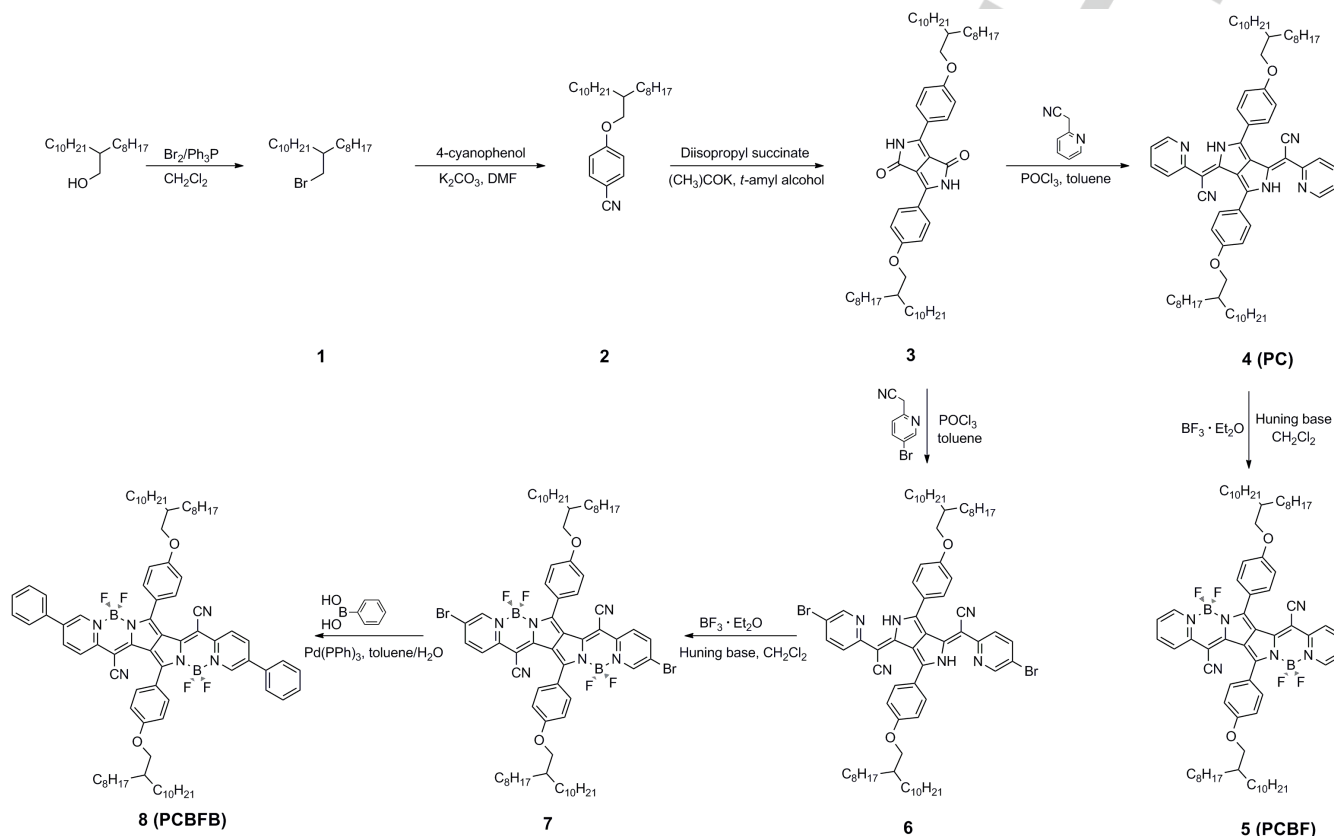
Dr. C. Xu
NTU-Northwestern Institute for Nanomedicine
Nanyang Technological University
50 Nanyang Avenue, Singapore 639798, Singapore
Dr. X. Wang (Present address)
National Center for Nano Science and Technology
Zhongguancun Beijiyitiao, Beijing 100190, China.

[†] These two authors contribute equally.

Supporting information for this article including detailed synthetic and preparation procedure and supporting figures is given.

To render the hydrophobic dye **PCBF** dispersible in water, a synthetic amphiphilic block copolymer PCL-*b*-POEGMA ($M_n = 31,100$; $M_w/M_n = 1.37$) was employed to encapsulate **PCBF** into the hydrophobic core of NPs via a process of nanoprecipitation (Scheme 1).^[7c] Both H-aggregation and J-aggregation of PCBF

occur in the corresponding NPs. These NPs exhibited bright NIR fluorescence, which is mainly contributed by J-aggregating components, and robust photostability that is important for bioimaging application.



Scheme 2 Synthetic route to Compound **PC**, **PCBF** and **PCBFB**.

Results and Discussion

The synthetic route to **PCBF** is illustrated in Scheme 2, using a modified method reported by Fischer and coworkers.^[13a] 3,6-Bis(4-octyldodecyloxyphenyl)-2,5-dihydropyrrolo [3,4-*c*]pyrrole-1,4-dione (Compound **3**, Scheme 2) was prepared by using a condensation of diisopropyl succinate 4-octyldodecyloxybenzotrile in the solution of potassium tert-butoxide and 2-methyl-2-butanol, where octyldodecyl branch group can provide DPP with a relatively good solubility. Subsequently, condensations of C-H acidic methylene groups from 2-cyanomethylpyridine at the carbonyl group of **3** proceeded in toluene with an excess of phosphoryl chloride to give compound **PC**, respectively. In order to stiffen the chromophores to activate NIR emission, trifluoroborane etherate was added to the dichloromethane solution of **PC** at the presence of Hünig base to give **PCBF** with a quantitative yield.

The UV-Vis-NIR absorption and FL emission spectra of **PCBF** in CHCl_3 (Figure 1a) show all the intrinsic features of PPcy. The

absorption maximum of monomeric **PCBF** appears at 700 nm (absorption coefficient: $\epsilon = 1.55 \times 10^5 \text{ cm}^{-1}\text{M}^{-1}$, even higher than that of porphyrin^[14]) while the FL emission spectrum exhibits a maximum at 715 nm. Thus PCBF in CHCl_3 shows a Stokes shift of 15 nm and a quite high FL quantum yield of 0.69 using ICG in water (QY~0.01) as a standard. The emission band is relatively broad with full-width-at-half-maximum (FWHM) value of 6910 cm^{-1} than that of absorption band (3849 cm^{-1}) (Figure 1a). The optical properties of PCBF observed here are consistent with what was reported by Fischer and coworkers.^[13]

In order to prepare colloidal NPs of **PCBF** in water, a mixture of **PCBF** and PCL-*b*-POEGMA codissolved in THF was rapidly injected into large excess water under ultrasonication, followed by evaporation of the organic solvent, resulting in colloidal stable NPs. Our previous work has demonstrated that the size of nanoparticles prepared by this nanoprecipitation method can be facilely tuned from 50 to 400 nm by varying the weight ratio of fluorophore/PCL-*b*-POEGMA.^[7c] In this work, a dispersion of NPs based on **PCBF** was obtained at a weight ratio of **PCBF**/PCL-*b*-POEGMA at 3.5 and a concentration of **PCBF** at 0.4 mM. As shown in Figure 1c, roseberry-like spherical NPs

with an average diameter of 30.0 ± 2.5 nm were observed in the transmission electron microscopy (TEM) image of JAGG NPs (Figure 1c). Beneficial from the higher electron density of **PCBF** than the PCL-*b*-POEGMA matrices, dye aggregation inside the NPs gave a clear contrast of **PCBF** aggregates as darker dots in the grey matrices of the polymeric NPs. The hydrodynamic diameter of JAGG NPs measured by dynamic light scattering (DLS) is 47.5 nm (Figure 1d), which is larger than that from TEM result due to the hydration of POEGMA corona.

In striking contrast to the optical absorption of monomeric **PCBF** in CHCl_3 , the JAGG NPs in water exhibit two new absorption bands as shown in Figure 1b. The blue-shifted band versus the monomeric band (M-band) appears as a typical signal of the formation of H-type and/or dimer aggregation (both are included as H-band here for simplification).^[15] The maximum of the H-aggregate absorption band (H-band) is centered at 647 nm. As compared to the M-band, another narrow and intense band in the absorption transition shows a 61 nm red-shift to 768 nm (Figure 1b), which is a spectral signature of ordered J-aggregates. Furthermore, the FWHM of J-band is narrower (2235 cm^{-1}) than that of **PCBF** in CHCl_3 (3849 cm^{-1}). This spectral-narrowing phenomenon is a known property of coherently coupled J-aggregates. It has been predicted that the absorption spectral width of the aggregate is narrower than that of the monomer by a factor $N^{1/2}$, where N is the number of monomers in direct communication with each other.^[16] The average J-aggregation number N calculated from the spectral narrowing of JAGG NPs is 7.4.

A control experiment was also conducted to monitor the formation of **PCBF** aggregates by varying the volume ratio of water/THF mixture in the absence of PCL-*b*-POEGMA. As shown in Figure S3a, with the gradual increase water fraction (f_w , by volume) from 0 to 40%, there is no significant change in the absorption spectra. Further increase of f_w to 50% led to the appearance of J-band, accompanied with a transition from transparent solution to suspension of aggregates which precipitated after standing overnight, implying the poor colloidal stability in the absence of the polymeric surfactant. The DLS histogram (Figure S3b) of the formed aggregated shows an average diameter of 10 μm , significantly larger than the size of the JAGG NPs stabilized by PCL-*b*-POEGMA. When f_w was increased to 60%, the J-band became stronger and sharper. The absence of H-band in the absorption spectra of the neat **PCBF** aggregates suggests the preferable formation of J-aggregation under the present experimental condition. The presence of the relatively high fraction of good solvent (i.e. THF) in the THF/water mixture might enable **PCBF** molecules to self-assemble to reach the more thermodynamically stable state, i.e. J-aggregation. In contrast, the aforementioned JAGG NPs were prepared by a rapid injection of a small amount of **PCBF**/THF solution (1 mL) into water (10 mL). The flash precipitation process may not allow all of the **PCBF** molecules to form J-aggregation immediately, resulting in the mixture of H-aggregates, J-aggregates and some **PCBF** monomers in JAGG NPs. In other words, the JAGG NPs described above represent a kinetically trapped or instantly frozen state in the nanoprecipitation process.

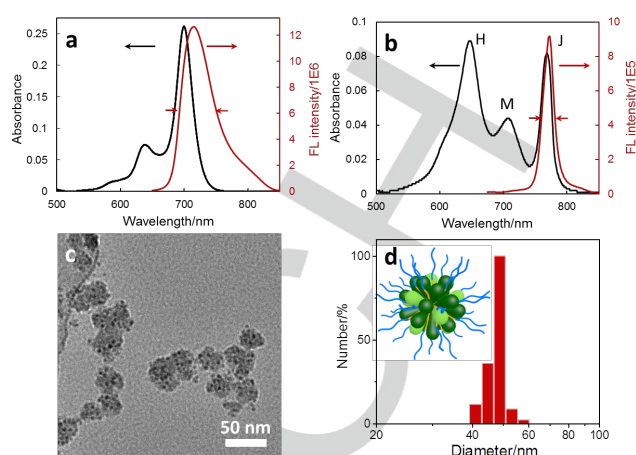


Figure 1 (a) UV-Vis-NIR absorption and FL emission spectra of **PCBF** in chloroform. (b) UV-Vis-NIR absorption and FL emission spectra of **PCBF** based JAGG NPs with the concentration of 0.4 mM in aqueous media. (c) TEM image of JAGG NPs of **PCBF** with the concentration of 0.4 mM in aqueous media; (d) DLS result shows the size distribution of JAGG NPs of **PCBF** in aqueous media.

The FL emission spectrum of JAGG NPs dispersion shows a characteristically small Stokes shift of 5 nm, a $\lambda_{\text{max,em}}$ of 773 nm and a smaller FWHM of 2114 cm^{-1} than that of **PCBF** in chloroform (6910 cm^{-1}) as shown in Figure 1b, which provides further evidence of J-aggregate formation. Evidently, the emission of monomeric molecules was not observed in Figure 1b. It can be explained by the intrinsic Förster resonance energy transfer (FRET) from monomer to J-aggregates in confined space due to the well overlapping between emission band of monomer (Figure 1a) and absorption band of J-aggregates (Figure 1b). The excitation spectrum (Figure S2) of JAGG dispersion at the emission wavelength of 773 nm shows emission maxima at the excitation wavelength of 769 nm, with an intensity approximately 35 times higher than that excited at 650 nm. This result suggests that the J-aggregates are the most active component that contributes to the fluorescence. While the calculated the FL quantum yield (0.012) of JAGG NPs excited at 650 nm in water is much lower than that (0.69) of **PCBF** in CHCl_3 , it is comparable with those of water-soluble PPcy derivatives (0.01)^[13c] and ICG (0.01)^[17] in water. It should be noted that the actual FL quantum yield of JAGG is underestimated here, given the fact that only a small fraction of light at 650 nm (i.e. the excitation wavelength) is absorbed by the J-aggregates. Due to the small Stokes shift (5 nm) of the emission band versus the absorption band of the J-aggregates, it is difficult to estimate the FL quantum yield of JAGG when the J-absorption band is excited. Nevertheless, the effect of the excitation wavelength on the FL intensity of the J-aggregates is reflected from the FL excitation spectrum shown in Figure S2.

The photostability of JAGG NPs under continuous irradiation with a 770-nm laser (power density $\sim 0.22 \text{ W/cm}^2$) was investigated using ICG in water as the control, where the absorbance at 770 nm of both JAGG and ICG was kept at 1.4. With the increase of irradiation time, the maximal absorbance

and FL emission intensity of ICG aqueous solution decreased quickly, accompanied by the color change of ICG solution from green to colorless (Figure 2a & 2b). In contrast, only negligible decrease of absorbance could be observed in JAGG solution under the same condition of irradiation (Figure 2c). After 55 min of continuous irradiation, the decrease of the FL intensity at 771 nm of JAGG solution was $\sim 12\%$ (Figure 2d), much lower than that (97%) at 805 nm of ICG solution, indicating relatively high photostability of JAGG NPs. The excellent photostability could be attributed to the intrinsic structural stability of PPcy^[13a] and its isolation from unfavorable influences of the environment.^[4b, 18] Hence, these JAGG NPs with such a large size are preferable for long-term tracking due to the increase of circulation half-life and excellent photostability compared to water-soluble dyes.^[18b, 19]

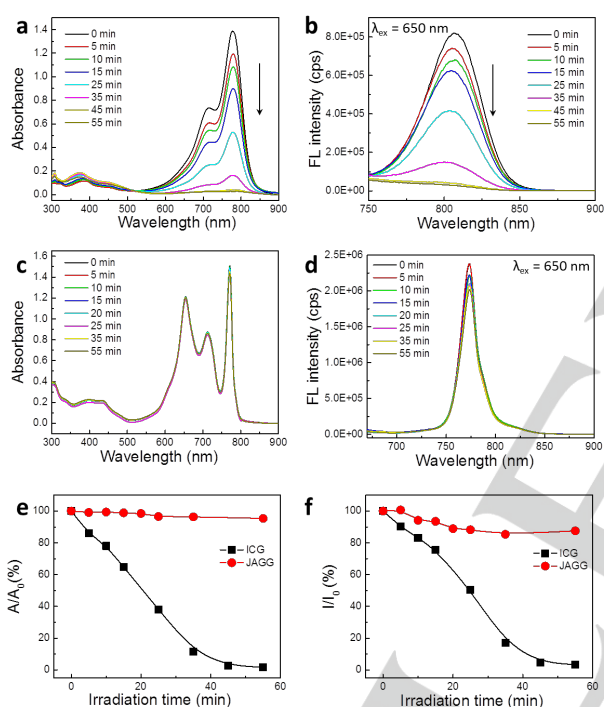


Figure 2 The evolution of UV-Vis-NIR absorption spectra (a) and FL emission spectra (b) of ICG solution in water under continuous irradiation by a 770 nm laser for ~ 1 h at a power density of 0.22 W/cm^2 ; UV-Vis-NIR absorption spectra (c) and FL emission spectra (d) of PCBF based JAGG dispersion under continuous irradiation by a 770 nm laser for ~ 1 h at a power density of 0.22 W/cm^2 ; (e) NIR absorbance ratio A/A_0 of ICG solution and JAGG dispersion plotted as a function of irradiation time. A_0 is the initial absorption maximum and A is the absorption maximum of the sample at different time points after illumination. (f) NIR fluorescence intensity ratio A/A_0 of ICG solution and JAGG dispersion plotted as a function of irradiation time. F_0 is the initial fluorescence maximum and F is the fluorescence maximum of the sample at different time points after illumination.

The effect of the concentration of PCBF and the weight ratio

of PCBF/PCL-*b*-POEGMA on the spectral characteristics were studied. We gradually decreased the feeding amount of PCBF when the amount of surfactant was kept constant. The concentration-dependent UV-Vis-NIR spectroscopy revealed that the J-aggregation in JAGG NPs was enhanced with the increase of the concentration of PCBF from 0.04 to 0.4 mM, accompanied by a gradually sharpening J-band and increasing ratio between J-band and H-band absorbance (Figure 3a & 3c). This result, as expected, indicates that formation of the J-aggregate was favoured by increased concentration of PCBF. With the increase of J-aggregate proportion, a slight 4 nm red-shift in the absorption from 764 to 768 nm was observed (Figure 3c). A shoulder peak at longer wavelength can be found in the J-aggregate absorption band of the JAGG dispersions at 0.04, 0.08 and 0.16 mM, respectively. Interestingly, the J-band in the absorption spectrum of the NPs at 0.24 mM exhibits two overlapping peaks at 766 and 771 nm, respectively (Figure 3c). This is a clear indication of the two overlapping bands of J-aggregation presumably due to two populations of J-aggregates with different geometrical configurations.^[20] Evidently, with the increase of PCBF concentrations from 0.04 to 0.4 mM, the intensity of the emission band with $\lambda_{\text{max,em}}$ at 773 nm gradually increased and the bandwidth turned narrower (Figure 3b), which is attributed to the increasing proportion of J-aggregation and configuration corresponding to the longer absorption wavelength

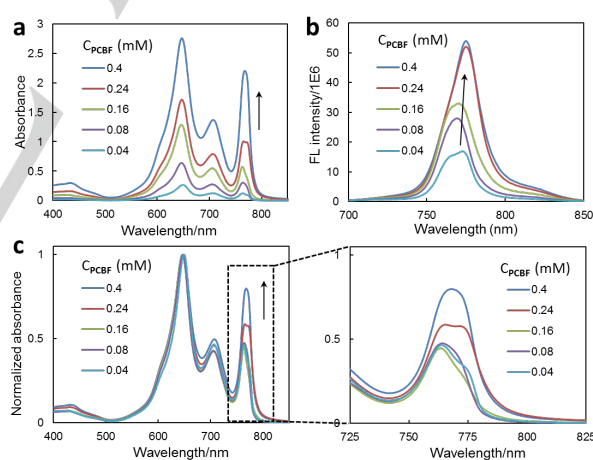


Figure 3 Concentration-dependent absorption spectra (a) and FL emission spectra (b) of PCBF based JAGG NPs upon the encapsulation of PCL-*b*-POEGMA. (c) Concentration-dependent normalized absorption spectra and zoom-in J-band variation of PCBF based JAGG NPs. C_{PCBF} corresponds to concentration of PCBF.

We envisioned that such unusual optical property of the J-aggregate of PCBF was encoded in its molecular structure: a planar conjugated core stiffened by difluoroborane group. To confirm this presumption, PC, the precursor of PCBF, was encapsulated by PCL-*b*-POEGMA to give colloidal dispersion as

a control. In contrast to **PCBF**, the absorption spectra of **PC** dispersion (Figure 4c) with 0.4 mM exhibited two peaks at 648 and 705 nm, which could be typically assigned to H-band and M-band, respectively. The same optical feature was observed at different concentrations of **PC** (Figure 4c & S8), suggesting no formation of J-aggregates. Such dramatically different aggregation behaviours between **PC** and **PCBF** may be rationalized by the more rigid and planar aromatic core and the resonance structure of a merocyanine in the latter, which favors the formation of J-aggregates.

To further understand how the structural details determine the aggregating state, **PCBFB** extended with two benzene rings was synthesized (Scheme 2). In contrast to **PCBF**, **PCBFB** showed a higher $\lambda_{\text{max,abs}}$ of 729 nm and $\lambda_{\text{max,em}}$ of 743 nm due to the extension of conjugation (Figure 4b). A high FL quantum yield (0.56) of **PCBFB** in CHCl_3 was also achieved. After encapsulation with PCL-*b*-POEGMA in water, the absorption spectra of **PCBFB** NPs (0.4 mM) exhibited the typical feature of H-aggregation (Figure 4d). **PCBFB** preferentially formed sandwich-type H-aggregates with significantly quenched fluorescence (quantum yield of 0.0011). The twist between the benzene ring and the PPcy core in **PCBFB** may reduce the planarity of the aromatic component as compared to **PCBF**. These results imply that the planarity and rigidity of the aromatic cores in **PCBF** could possibly facilitate the formation of J-aggregates. Nevertheless, a clear picture how **PCBF** molecules stack inside the colloidal nanoparticles remains unclear, and warrants further experimental study, for example, of the crystalline structures of PPcy derivatives and some simulation study in the future.

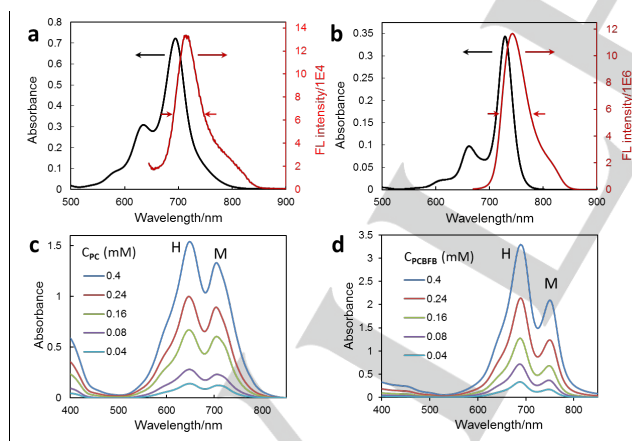


Figure 4 (a) UV-Vis-NIR absorption and FL emission spectra of **PC** in chloroform. (b) UV-Vis-NIR absorption and FL emission spectra of **PCBFB** in chloroform. Concentration-dependent absorption spectra of (c) **PC** and (d) **PCBFB** based JAGG NPs upon the encapsulation of PCL-*b*-POEGMA. C_{PC} and C_{PCBFB} correspond to concentration of **PC** and **PCBFB** in stock solutions. (All the samples were diluted by eight folds before test)

The optical properties of several kinds of J-aggregates based on supramolecular assembly have been reported to be tunable

by changing the environmental temperature.^[12, 21] In contrast, as shown in Figure S10, only a slight change around J-band was observed in the UV-Vis-NIR absorption spectra of JAGG dispersion (0.4 mM) with the gradually increased temperature from 25 to 60 °C.

We previously reported that ultrasonication played a role to induce the colloidal crystallization of an indigo derivative.^[22] Here, the colloidal NPs of **PCBF** were also treated with ultrasonication. Upon the ultrasonic treatment for 200 mins, the absorbance of J-band at 774 nm gradually increased, accompanied with the decrease of H-band absorbance (Figure 5a). The change can be observed with naked eyes, as the bluish solution of JAGG NPs turned green upon ultrasonication (Figure 5a). These results clearly indicate the transition from H-aggregate to J-aggregate.^[10] Moreover, the J-band in the absorption spectra exhibits a red-shift of 6 nm (from 768 to 774 nm) upon ultrasonication for 200 mins while the FL emission spectrum shows a $\lambda_{\text{max,em}}$ of 774 nm and negligible Stokes shift (Figure 5b & 5c). The FL quantum yield of JAGG NPs after ultrasonication for 200 mins was increased to 0.025, consistent with the increase of J-aggregate population. It is noted that there was no obvious change of the morphology and the size of JAGG after the ultrasonication (Figure 5d & Figure S11).

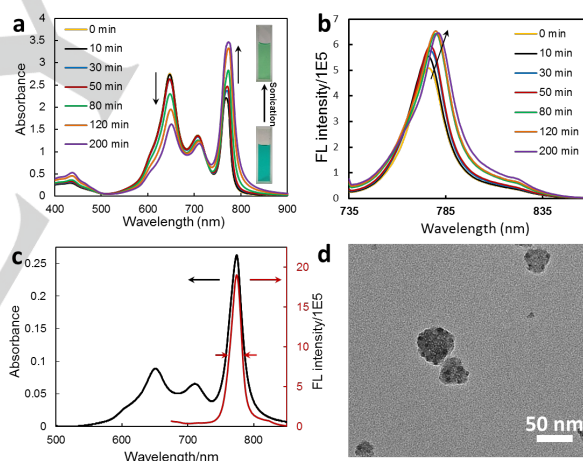


Figure 5 The evolution of UV-Vis-NIR spectra (a) and FL emission spectra (b) of **PCBF**-based JAGG NPs (diluted by eight folds from 0.4 mM stock solution with water) after ultrasonication over different periods; arrows indicate the spectroscopic changes with increasing ultrasonication time. (c) UV-Vis-NIR absorption and FL emission spectra of **PCBF** based JAGG NPs after sonication for 200 mins. (d) TEM image of **PCBF** based JAGG NPs after sonication for 200 mins.

The optical properties of JAGG NPs described above, meeting most requirements of a FL imaging probe, encouraged us to examine their potential for *in vivo* imaging. Firstly, the cytotoxicity of JAGG NPs against mouse fibroblast cells (L929) was studied by PrestoBlue assays. As summarized in Figure 6a, there was no obvious change of the metabolic viability of L929 cells after incubation with JAGG for 72 h at a series of concentrations of 0.01, 0.02, 0.05, 0.1, 0.2 mM, respectively,

indicating the low cytotoxicity of JAGG NPs. In *in vivo* experiment, subcutaneous and intramuscular injections of JAGG dispersions (50 μ L aliquots, 1 mg/mL) into the left flank (position II in Figure 6b) and left leg (position III in Figure 6b) of a nude mouse, respectively, were administered. The mouse was imaged in a fluorescence mode (excitation filter, 605-640 nm, and emission filter, 740-800 nm). The FL signals collected from both injected regions were clearly observed and the FL intensity emanating from deeper tissue (ROI (III) = 9.856×10^{10} , ROI stands for regions of interest) is comparable with that of the near-skin fluorescence (ROI (I) = 1.029×10^9) (Figure S12). As a control, the HAGG dispersion of **PCBFB** was subcutaneously and intramuscularly injected to right flank (position IV) and right leg (position V), respectively (Figure 6b). Obviously, the weak fluorescence signals (ROI (IV) = 5.340×10^8 ; ROI (V) = 5.492×10^8) observed here were only slightly stronger than that of the blank (ROI (I) = 1.571×10^8), due to the quite low FL quantum yield of the **PCBFB** NPs.

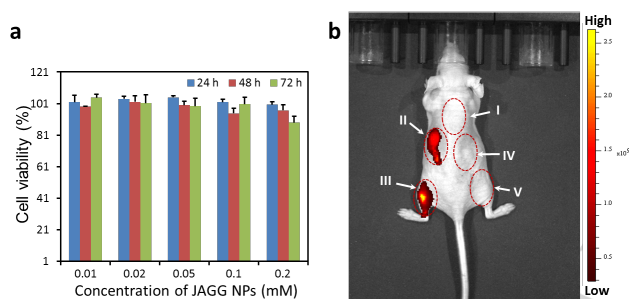


Figure 6 (a) Metabolic viability of L929 cancer cells after incubation with JAGG NPs at different concentrations. (b) *In vivo* fluorescence image of JAGG and HAGG NPs (50 μ L of 1 mg/mL) injected subcutaneously and intramuscularly on each flank of a mouse. Position I: blank control; II: JAGG NPs subcutaneous; III: JAGG NPs intramuscular; IV: HAGG NPs subcutaneous; V: HAGG NPs intramuscular.

Conclusions

In summary, we have presented a novel type of colloidal NPs based on the J-aggregation of PPcy dyes stabilized with a polymeric surfactant in water. The packing configuration of PPcy in NPs is determined by factors including the chemical structure, the concentration of the dye and the ultrasonication treatment. The outstanding spectroscopic properties of JAGG NPs, such as large light-absorption coefficient, relatively high FL quantum yield, as well as narrow emission band, enable them to be promising candidates for *in vivo* imaging in the near infrared range. These JAGG NPs may also be useful for multimodal imaging (fluorescence and photoacoustic)^[11a] and therapeutic (photothermal therapy) applications.^[23]

Experimental Section

Materials

10 \times phosphate buffer saline (PBS) buffer with pH = 7.4 (ultrapure grade) is a commercial product of 1st BASE Singapore. MilliQ water (18.2 MQ) was used to prepare the buffer solution from the 10 \times PBS stock buffer. 1 \times PBS consists of NaCl (137 mM), KCl (2.7 mM), Na₂HPO₄ (10 mM) and KH₂PO₄ (1.8 mM). Chloroform-D (99%) was purchased from Cambridge Isotope Laboratories, Inc. All other chemicals and reagents were purchased from Aldrich or Merck and used as received unless other specified. Block copolymers PCL-*b*-POEGMA was obtained according to our previous work.^[7c]

Characterization

The samples were dissolved with chloroform-d for ¹H NMR and ¹³C NMR measurements on a Bruker AV300 MHz NMR spectrometer. Emission spectra of solutions were measured by fluorescence spectrophotometry on a Horiba Fluolog 3 spectrofluorometer at 25 $^{\circ}$ C. The fluorescence quantum yield of these materials were measured using indocyanine green (ICG) solution in water as the standard ($\Phi_F = 0.01$). UV-Vis-NIR spectra of the samples were measured on a SHIMADZU UV-2450 spectrophotometer. The photostability of ICG solution and JAGG dispersion subjected to the continuous irradiation by a 770 nm laser (power density ~ 0.22 W/cm²) over different periods was monitored by the UV-Vis spectrometer and fluorometer. TEM measurements were performed with a TEM Carl Zeiss Libra 120 Plus at an acceleration voltage of 120 kV. A 5 μ L droplet of diluted samples was directly dropped onto a copper grid (300 mesh) coated with a carbon film, followed by drying at room temperature. The size distribution of resulting nanoparticles were determined by dynamic light scattering (DLS) using a BI-200SM (Brookhaven, USA) with angle detection at 90 $^{\circ}$. Ultrasonic treatment of JAGG dispersion was performed in an ultrasonic cleaner (SB-120 DTN, power: 120 W) bath. Temperature-dependent variation on absorption spectra of JAGG dispersions was monitored by the UV-Vis spectrometer from 25 to 60 $^{\circ}$ C. Each temperature point was kept for 1 h to treat the sample.

Synthesis of Compound 1

Triphenylphosphine (26 g, 0.1 mol) was dissolved in dichloromethane (100 mL). Then, bromine (16 g, 0.1 mol) was added dropwise at 0 $^{\circ}$ C. After completion of adding bromine, the reaction mixture was stirred half an hour at room temperature. 2-octyl-1-dodecanol (30 g, 0.1 mol) was added slowly. The reaction mixture was stirred at room temperature overnight. Then the reaction mixture was poured into water (200 mL) and extracted with dichloromethane (3 \times 50 mL). The extracts were combined and washed with water and saturate sodium bicarbonate solution then dried over anhydrous magnesium sulfate. After filtration, filtrate was concentrated to 100 mL under reduced pressure. Petroleum ether (200 mL) was added to the mixture and stirred. Resulting triphenylphosphine oxide precipitate was filtered off and filtrate was concentrated to 100

ml. Added another 100 mL petroleum ether and filtered. Repeated this operation till no precipitate observed, and the filtrate was evaporated to dryness. The product 2-octyl-1-dodecyl bromide was obtained in a yield of 92% and used in subsequent reactions without further purification.

Synthesis of Compound 2

4-Cyanophenol (1.19 g, 10 mmol) and potassium carbonate (5.52 g, 40 mmol) were dissolved in 60 ml acetone. After being purged for 15 min, the mixture was heated to 100 °C for half an hour. Then, 2-octyl-1-dodecyl bromide (4 g, 11 mmol) was added to the mixture by syringe. The reaction mixture was stirred at 100 °C for 30 h. After cooled to room temperature, the reaction mixture was added to 100 mL of water and extracted with ethyl acetate. The extracts were combined and washed with water then dried over anhydrous magnesium sulfate. The crude product was purified by flash chromatography (petroleum ether/dichloromethane from 10: 0 to 10:1) to yield target product as a light yellow viscous liquid in a yield of 90%. ¹H NMR (300 MHz, CDCl₃): 7.58 (2H, d), 6.97 (2H, d), 3.88 (2H, d), 1.81 (1H, m), 1.25-1.50 (32H, broad), 0.90 (6H, t).

Synthesis of Compound 3

Potassium tert-butoxide (1.68 g, 15 mmol) was added to 2-methyl-2-butanol 15 mL, and the mixture was heated to reflux. When the alkali is dissolved, Compound 2 (4 g, 10 mmol) was added in one portion. Then diisopropyl succinate (1.01 g, 5 mmol) was added over three hours with a dropping funnel. After heated for another three hours at 110 °C, the mixture was cooled down and slowly added to a mixture of 100 mL ethanol (containing 2 mL concentrated hydrochloric acid). The red precipitate is filtered and washed with ethanol. The solid is digested in boiling ethanol, filtered and washed with ethanol. This procedure is repeated until the filtrate is clear. Drying in vacuum yields 2.1 g (24 %) orange solid. ¹H NMR (300 MHz, CDCl₃): 8.42 (2H, s), 8.26 (4H, d), 7.08 (4H, d), 3.96 (4H, d), 1.84 (2H, m), 1.25-1.50 (64H, broad), 0.90 (12H, m).

Synthesis of Compound 4

Compound 3 (0.88 g, 1 mmol) and 2-cyanomethylpyridine or 2-cyanomethylpyridine (0.295 g, 2.5 mmol) or were heated to reflux in absolute toluene (20 mL) under nitrogen. Phosphoryl chloride (0.75 ml, 8 mmol) was then added. The reaction was monitored by thin-layer chromatography. As soon as 3 was used up, the reaction mixture was cooled down, quenched by water and alkalize by sodium bicarbonate solution. Water was separated and extracted with chloroform. The combined organic layer was dried over anhydrous sodium sulfate. After filtration, the volatiles were removed under reduced pressure. The crude product was purified by column chromatography on silica, eluting with dichloromethane/petroleum ether (from 1:5 to 1:1) to give Compound 4 as a bluish green solid (173 mg, 16%). ¹H NMR (300 MHz, CDCl₃): 13.6 (2H, s), 8.45 (2H, d), 7.65 (8H, m),

7.12 (4H, d), 7.01 (2H, t), 3.97 (4H, d), 1.84 (2H, m), 1.25-1.50 (64H, broad), 0.89 (12H, m).

Synthesis of Compound 5

Compound 4 (25 mg, 0.02 mmol) and N,N-diisopropylethylamine (0.2 mL, 1.2 mmol) were dissolved in dichloromethane (2 ml). Trifluoroborane etherate (0.2 mL, 1.6 mmol) was added and the mixture was stirred at room temperature for 2 hours. The reaction mixture was washed with water and dried over anhydrous sodium sulfate. After removing the solvent, the crude product was purified by column chromatography, eluting with dichloromethane to give Compound 5 as a green solid (26 mg, quantitative yield). ¹H NMR (300 MHz, CDCl₃): 8.36 (2H, d), 7.88 (2H, t), 7.65 (6H, m), 7.22 (2H, t), 7.08 (4H, d), 3.95 (4H, d), 1.83 (2H, m), 1.25-1.50 (64H, broad), 0.91 (12H, m).

Synthesis of Compound 7

5-bromo-2-cyanomethylpyridine was used to replace 2-cyanomethylpyridine as the raw materials. The procedure to synthesize 8 was similar with that of 2 and the similar yield was achieved. ¹H NMR (300 MHz, CDCl₃): 8.43 (2H, d), 7.91 (2H, d), 7.64 (4H, d), 7.55 (2H, d), 7.07 (4H, d), 3.95 (4H, d), 1.83 (2H, m), 1.25-1.50 (64H, broad), 0.91 (12H, m).

Synthesis of Compound 8

Compound 8 (133.5 mg, 0.1 mmol), phenylboronic acid (36.6 mg, 0.3 mmol) and K₂CO₃ (1.38g) was dissolved in degassed mixture of toluene (10 mL), water (2 mL) and ethanol (2 mL) under nitrogen atmosphere. It is followed by addition of a catalytic amount (1% m/m) of Pd(PPh₃)₄. The resulting mixture was heated at 100 °C for 6 h, then cooled down to room temperature. The organic layer was washed by water for three times and concentrated under reduced pressure. The product was purified by column chromatography on silica using dichloromethane/hexane (1/1) as the solvent and dried under vacuum at 80 °C overnight. Finally, we obtained 121.4 mg dark green powder (yield 91.3%). ¹H NMR (300 MHz, CDCl₃): 8.61 (2H, s), 8.09 (2H, d), 7.70 (6H, m), 7.49 (10H, m), 7.10 (4H, d), 3.96 (4H, d), 1.84 (2H, m), 1.25-1.50 (64H, broad), 0.90, (12H, m).

Preparation of nanoparticles in the presence of surfactant as stabilizer

Taking JAGG NPs with 0.4 mM as representative example, PCBF (200 μL×0.01M THF solution) and amphiphilic copolymer PCL-*b*-POEGMA (100 μL×6.67 g/L THF solution) were mixed in 200 μL of THF. This mixture was rapidly injected into 5 mL of deionized water under ultrasonication. THF was evaporated by exposure in open air overnight. Similarly, JAGG dispersions with concentration of 0.24, 0.16, 0.08 and 0.04 mM were prepared by using 120, 80, 40 and 20 μL of 0.01M THF solution of PCBF, respectively, while the amount of PCL-*b*-POEGMA was kept unchanged. HAGG dispersions with various concentrations were obtained by the similar procedure.

Monitoring the aggregation of PCBF in mixture of THF/water in the absence of surfactant as stabilizer

An aliquot of **PCBF** (100 μ L, 1 mg/mL in THF) was mixed with different amounts of THF (x mL), followed by a quick addition of a known volume of water ((3-x) mL) and mixed with gentle shaking. Through this process, a series of **PCBF** dispersions were obtained with different water fractions (f_w = 0%, 10%, 20%, 30%, 40%, 50%, 60% by volume).

Cell culture and cytotoxicity study

L929 mouse fibroblast cells were cultured in folate-free Dulbecco's Modified Eagle's Medium (DMEM) containing 10% fetal bovine serum and 1% penicillin streptomycin at 37 °C in a humidified environment containing 5% CO₂. Before experiments, the cells were precultured until confluence was reached. The cytotoxicity of JAGG NPs against L929 cancer cells was evaluated by PrestoBlue (PB) assay. Briefly, L929 cells were seeded in 96-well plates (Costar, IL, USA) at an intensity of 5×10^4 cells mL⁻¹. After 12 h incubation, the cells were exposed to a series of doses of JAGG NPs at 37 °C. After the designated time intervals, the wells were washed twice with 1×PBS buffer and 100 μ L of freshly prepared PB solution in culture medium was added into each well. The PB medium solution was carefully removed after 1 h incubation in the incubator. The absorbance of PB at 570 nm and 600 nm was monitored by the microplate reader (Genios Tecan). Cell viability was expressed as the ratio of the percent PB reduction of the cells incubated with JAGG NPs suspension to that of the cells incubated with culture medium only.

In vivo fluorescence imaging

The care and use of laboratory animals were performed according to the approved protocols of the Institutional Animal Care and Use Committee (IACUC) at Nanyang Technological University, Singapore. 50 μ L of JAGG solution of **PCBF** and HAGG solution of **PCBFB** (1 mg/ml) were subcutaneously injected to the left or right side of flanks of 8-week-old NCr nude mice (Invivos Pte Ltd), respectively. Next, 50 μ L of the same JAGG dispersion of **PCBF** and HAGG dispersion of **PCBFB** were intramuscularly injected to left or right side of rear legs, respectively. The efficacy of dye as imaging agents was then examined using an IVIS SpectrumCT *in vivo* imaging system (PerkinElmer). The wavelengths of excitation and emission filters used were 605-640 nm, and 740-800 nm, respectively. The auto-fluorescence of the skin was removed using a spectral unmixing software.

Acknowledgements

MW is grateful to the funding support by a start-up grant (M4080992.120) of Nanyang Assistant Professorship from Nanyang Technological University, AcRF Tier 2 (ARC 36/13) from the Ministry of Education, Singapore. XCJ also

acknowledges the financial support from NTU-Northwestern Institute for Nanomedicine (M4081502.F40). We thank Dr. Hongwei Duan for access to the fluorometer. We also thank Dr. Quan Liu and Mr. Xiang Li for the assistance in the use of the 770-nm laser.

Keywords: J-aggregates • Near-infrared • Fluorescence • Pyrrolopyrrole Cyanines • Bioimaging

- [1] (a) E. M. Sevick-Muraca, J. P. Houston, M. Gurfinkel, *Curr. Opin. Chem. Biol.* **2002**, *6*, 642-650; (b) J. V. Frangioni, *Curr. Opin. Chem. Biol.* **2003**, *7*, 626-634.
- [2] A. L. Vahrmeijer, M. Hutteman, J. R. van der Vorst, C. J. van de Velde, J. V. Frangioni, *Nat. Rev. Clin. Oncol.* **2013**, *10*, 507-518.
- [3] H. Maeda, *Bioconjugate Chem.* **2010**, *21*, 797-802.
- [4] (a) M. J. Pittet, F. K. Swirski, F. Reynolds, L. Josephson, R. Weissleder, *Nat. Protoc.* **2006**, *1*, 73; (b) S. Huang, S. Liu, K. Wang, C. Yang, Y. Luo, Y. Zhang, B. Cao, Y. Kang, M. Wang, *Nanoscale* **2015**, *7*, 889-895.
- [5] (a) H. Cabral, Y. Matsumoto, K. Mizuno, Q. Chen, M. Murakami, M. Kimura, Y. Terada, M. R. Kano, K. Miyazono, M. Uesaka, N. Nishiyama, K. Kataoka, *Nat. Nanotech.* **2011**, *6*, 815-823; (b) J. Wang, W. Mao, L. L. Lock, J. Tang, M. Sui, W. Sun, H. Cui, D. Xu, Y. Shen, *ACS Nano* **2015**, *9*, 7195-7206.
- [6] J. D. Luo, Z. L. Xie, J. W. Y. Lam, L. Cheng, H. Y. Chen, C. F. Qiu, H. S. Kwok, X. W. Zhan, Y. Q. Liu, D. B. Zhu, B. Z. Tang, *Chem. Commun.* **2001**, 1740-1741.
- [7] (a) S. Huang, K. Wang, S. Wang, Y. Wang, M. Wang, *Adv. Mater. Interfac.* **2016**; (b) K. Wang, Y. Luo, S. Huang, H. Yang, B. Liu, M. Wang, *J. Polym. Sci., Part A: Polym. Chem.* **2015**, *53*, 1032-1042; (c) C. Yang, H. Liu, Y. Zhang, Z. Xu, X. Wang, B. Cao, M. Wang, *Biomacromolecules* **2016**, *17*, 1673-1683.
- [8] (a) E. E. Jelley, *Nature* **1936**, *138*, 1009-1010; (b) G. Scheibe, *Angew. Chem.* **1936**, *49*, 563; (c) E. E. Jelley, *Nature* **1937**, *139*, 631-632; (d) G. Scheibe, *Angew. Chem. Int. Ed. Eng.* **1937**, *50*, 212-219.
- [9] (a) A. Herz, *Adv. Colloid Interface Sci.* **1977**, *8*, 237-298; (b) D. Möbius, *Adv. Mater.* **1995**, *7*, 437-444; (c) F. Würthner, T. E. Kaiser, C. R. Saha - Möller, *Angew. Chem. Int. Ed. Eng.* **2011**, *50*, 3376-3410; (d) S. Sengupta, F. Würthner, *Acc. Chem. Res.* **2013**, *46*, 2498-2512.
- [10] F. Rotermund, R. Weigand, A. Penzkofer, *Chem. Phys.* **1997**, *220*, 385-392.
- [11] (a) J. F. Lovell, C. S. Jin, E. Huynh, H. Jin, C. Kim, J. L. Rubinstein, W. C. Chan, W. Cao, L. V. Wang, G. Zheng, *Nat. Mater.* **2011**, *10*, 324-332; (b) M. Shakiba, K. K. Ng, E. Huynh, H. Chan, D. M. Charron, J. Chen, N. Muhanna, F. S. Foster, B. C. Wilson, G. Zheng, *Nanoscale* **2016**, *8*, 12618-12625; (c) K. K. Ng, M. Takada, C. C. Jin, G. Zheng, *Bioconjugate Chem.* **2015**, *26*, 345-351.
- [12] T. E. Kaiser, H. Wang, V. Stepanenko, F. Würthner, *Angew. Chem. Int. Ed. Eng.* **2007**, *46*, 5541-5544.
- [13] (a) G. M. Fischer, A. P. Ehlers, A. Zumbusch, E. Daltrozzo, *Angew. Chem. Int. Ed. Eng.* **2007**, *46*, 3750-3753; (b) G. M. Fischer, M. Isomäki - Krondahl, I. Göttker - Schnetmann, E. Daltrozzo, A. Zumbusch, *Chem. Eur. J.* **2009**, *15*, 4857-4864; (c) S. Wiktorowski, C. Rosazza, M. J. Winterhalder, E. Daltrozzo, A. Zumbusch, *Chem. Commun.* **2014**, *50*, 4755-4758; (d) G. M. Fischer, E. Daltrozzo, A. Zumbusch, *Angew. Chem. Int. Ed. Eng.* **2011**, *50*, 1406-1409; (e) G. M. Fischer, C. Jüngst, M. Isomäki-Krondahl, D. Gauss, H. M. Möller, E. Daltrozzo, A. Zumbusch, *Chem. Commun.* **2010**, *46*, 5289-5291.
- [14] K. K. Ng, M. Shakiba, E. Huynh, R. A. Weersink, A. Roxin, B. C. Wilson, G. Zheng, *ACS Nano* **2014**, *8*, 8363-8373.
- [15] (a) W. West, S. Pearce, *J. Phys. Chem.* **1965**, *69*, 1894-1903; (b) F. Würthner, Y. Sheng, B. Uwe, *Angew. Chem. Int. Ed. Eng.* **2003**, *42*, 3247-3250; (c) C. Shao, M. Grüne, M. Stolte, F. Würthner, *Chem. Eur. J.* **2012**, *18*, 13665-13677; (d) F. Würthner, *Acc. Chem. Res.* **2016**, *49*, 868-876.
- [16] E. Knapp, *Chem. Phys.* **1984**, *85*, 73-82.
- [17] S. A. Soper, Q. L. Mattingly, *J. Am. Chem. Soc.* **1994**, *116*, 3744-3752.
- [18] (a) H. S. Muddana, T. T. Morgan, J. H. Adair, P. J. Butler, *Nano Lett.* **2009**, *9*, 1559-1566; (b) E. I. Altinoğlu, T. J. Russin, J. M. Kaiser, B. M. Barth, P. C. Eklund, M. Kester, J. H. Adair, *ACS Nano* **2008**, *2*, 2075-2084.
- [19] J. Devoisselle, S. Soulie-Begu, S. Mordon, T. Desmettre, H. Maillols, *Laser. Med. Sci.* **1998**, *13*, 279-282.
- [20] (a) W. Cooper, *Chem. Phys. Lett.* **1970**, *7*, 73-77; (b) D. Eisele, C. Cone, E. Bloemsma, S. Vlaming, C. van der Kwaak, R. J. Silbey, M. G. Bawendi, J. Knoester, J. Rabe, D. V. Bout, *Nat. Chem.* **2012**, *4*, 655-662.

- [21] (a) X. Q. Li, X. Zhang, S. Ghosh, F. Würthner, *Chem. Eur. J.* **2008**, *14*, 8074-8078; (b) V. Huber, M. Katterle, M. Lysetska, F. Würthner, *Angew. Chem. Int. Ed. Eng.* **2005**, *117*, 3208-3212.
- [22] C. Yang, Q. T. Trinh, X. Wang, Y. Tang, K. Wang, S. Huang, X. Chen, S. H. Mushrif, M. Wang, *Chem. Commun.* **2015**, *51*, 3375-3378.
- [23] (a) S. Huang, P. K. Upputuri, H. Liu, M. Pramanik, M. Wang, *J. Mater. Chem. B* **2016**, *4*, 1696-1703; (b) S. Huang, R. K. Kannadorai, Y. Chen, Q. Liu, M. Wang, *Chem. Commun.* **2015**, *51*, 4223-4226.

WILEY-VCH

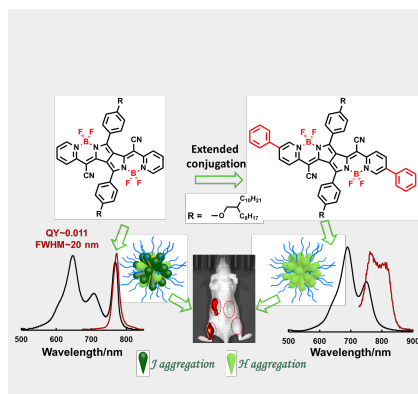
Accepted Manuscript

Entry for the Table of Contents (Please choose one layout)

Layout 1:

FULL PAPER

A novel class of colloidal nanoparticles containing near-infrared fluorescent J-aggregates of pyrrolopyrrole cyanines (PPcys) exhibit a narrow emission band at 773 nm, a fluorescence quantum yield comparable to that of indocyanine green, and significantly enhanced photostability that is ideal for long-term bioimaging.



Cangjie Yang, Xiaochen Wang,
Mingfeng Wang*, Keming Xu, Chenjie
Xu

Page No. – Page No.

**Robust Colloidal Nanoparticles of
Pyrrolopyrrole Cyanines J-
Aggregates with Bright Near Infrared
Fluorescence in Aqueous Media:
From Spectral Tailoring to
Bioimaging Application**